

## APPLICATION OF MODELS FOR IGSCC INSPECTION

T. A. Gray, R. B. Thompson and B. P. Newberry

Ames Laboratory, USDOE  
Iowa State University  
Ames, IA 50011

and

J. D. Achenbach and D. Budreck

Department of Civil Engineering  
Northwestern University  
Evanston, IL 60201

### INTRODUCTION

Ultrasonic detection and sizing of intergranular stress corrosion cracks (IGSCC) in nuclear reactor cooling systems is a difficult practical problem due to the complicated geometry of these defects and to the variety of other reflectors (e.g., welds) which produce competing ultrasonic indications. The use of models of scattering from such defects can help in improving physical insight into ultrasonic scattering from IGSCC's and may ultimately be of use in defining inspection protocols and signal processing algorithms which can lead to improved inspection reliability and discrimination between IGSCC's and other geometrical reflectors. This paper will discuss the application of a model of ultrasonic scattering from a simple Y-shaped crack based upon the Kirchhoff approximation. In this model, the ultrasonic beam is approximated by a Gaussian profile which includes the effects of diffraction and allows calculation of the full ultrasonic radiation pattern which may be used, for example, to simulate a scanned inspection. Included in this paper will be a brief description of the model and a presentation of simulated IGSCC results. Comparisons of the model to experimental measurements will then be addressed followed by an application to the problem of IGSCC sizing based upon the dB-drop and PAT (pulse-arrival-time) techniques.

### MODEL SUMMARY

The basis of the IGSCC model is an electromechanical reciprocity relationship which relates the ultrasonic fields in the vicinity of the flaw to the signals that could be received in a practical inspection[1]. Initially based upon a 2-D scattering model, recent work has extended the previously reported results[2] to allow the crack to have finite length[3]. The model 3-D Y-shaped crack is illustrated in Fig. 2(b) of Ref. 4. The main stem of the crack is a truncated semi-ellipse and the branches are semi-ellipses. The inspection configuration, shown in Fig. 1, is 45-degree shear

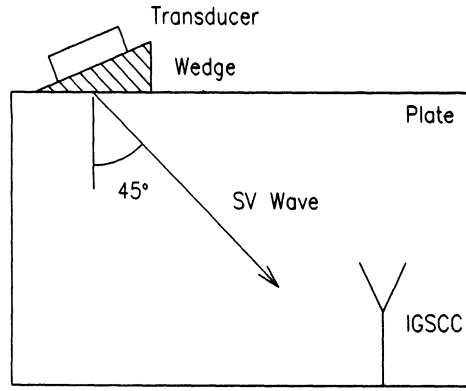


Fig. 1. Inspection configuration for Y-crack model.

wave backscatter. The ultrasonic beam is represented by a Gaussian beam model[5] which includes the effects of diffraction (beam spread) and allows computation of the full fields in order to simulate a scanned inspection. Scattering from the simulated IGSCC is described by a Kirchhoff approximation in which the ultrasonic fields which illuminate and scatter from the branches and stem are computed according to the Gaussian beam theory. The resulting model can be expressed in the following dimensionless form[3]:

$$\frac{HP\delta\Gamma}{2(U_o T_{o1})^2 \mu c_T f} = \frac{ik_T H}{8f} \iint_{A^+} \frac{\Delta u_i [(\tau_{i2}^{tr})^d + (\tau_{i2}^{tr})^r]}{(U_o T_{o1})^2 \mu} n_2 dx_1 dx_3. \quad (1)$$

The various terms in Eq. 1 are:

- H = plate thickness;
- P = electrical power incident on the transducer;
- $\delta\Gamma$  = variation of electrical reflection coefficient due to presence of a flaw;
- $U_o$  = maximum displacement of transducer face;
- $T_{o1}$  = wedge/plate ultrasonic transmission coefficient;
- $\mu$  = shear modulus;
- $c_T$  = shear velocity;
- f = surface breaking half-length of crack stem;
- $A^+$  = illuminated surface of crack;
- $k_T$  = shear wavenumber;
- $\Delta u_i$  = crack opening displacement;
- $\tau_{ij}$  = stress fields induced by the transducer with no flaw present, superscript refers to illumination by direct or reflected rays;
- $n_j$  = unit vector normal to crack surface.

In the current model implementation, the crack opening displacement and stress fields are approximated by assuming that the local illuminating fields on the branches or stem of the crack can be replaced by a plane wave whose amplitude is defined by the Gaussian beam theory evaluated at a user-specified point on the crack element. This represents a simplification of the actual scattering phenomena, but allows fast computation time, since the model, as indicated in Eq. 1, requires a double integration over the crack face. For plane waves, the integrals can be evaluated analytically.

Equation 1 is, in effect, an "impulse response" spectrum which is independent of the frequency characteristics of a particular transducer. To simulate a signal that might be measured in a practical situation, Eq. 1 must be convolved with an appropriate transducer frequency response. To illustrate this, it is convenient first to rewrite Eq. 1 as

$$\delta\Gamma = N \left[ \frac{(2f) \cdot c_T^2}{\omega^2 H \cdot A} \right] \left[ \frac{\rho c_T \omega^2 (U_o T_{o1})^2 A}{P} \right] \quad (2)$$

where N denotes the dimensionless quantity of Eq. 1 and A is the cross-sectional area of the ultrasonic beam. Note that the final term in Eq. 2 is a dimensionless power conversion efficiency term representing the acoustic power transmitted into the bulk of the plate per unit incident electrical power for a specific transducer.

This term can be determined by a reference measurement, e.g., the reflection from a corner of a plate identical to that containing the IGSCC. This reference signal can be expressed as

$$\delta\Gamma_R = D \left[ \frac{\rho c_T \omega^2 (U_o T_{o1})^2 A}{P} \right] \quad (3)$$

where D is a term to account for diffraction loss (beam spread). Equation 3 can be solved for the efficiency factor which is then inserted into Eq. 2 to yield

$$\delta\Gamma = N \cdot \delta\Gamma_R \frac{(2f)c_T^2}{D\omega^2 H \cdot A} \quad (4)$$

Experimentally, one measures a voltage rather than a reflection coefficient. However, since the proportionality between the two is the same for both the scattering and reference measurements,  $\delta\Gamma$  and  $\delta\Gamma_R$  in Eq. 4 may be interpreted as the measured signals.

Some means for computing the diffraction term D and the ultrasonic beam area A in Eq. 4 must be determined. In the following, the latter factor is approximated as the refracted elliptical "footprint" of the beam in the plate. Thus,

$$A = \pi a^2 \frac{\cos\theta_1}{\cos\theta_o} \quad (5)$$

where a is the probe radius and  $\theta_o, \theta_1$  are the angles of the beam in the wedge and in the plate relative to normal to the plate surface. The diffraction loss term D is approximated in an ad hoc manner by a formula which is valid for circular piston probes at normal incidence to the sample surface[6],

$$D(s) = 1 - e^{-i2\pi/s} (J_0(2\pi/s) + iJ_1(2\pi/s)) \quad (6)$$

where

$$s = 2 \left( \frac{z_0 \lambda_0}{a^2} + \frac{z_1 \lambda_1}{a^2} \right) \quad (7)$$

$\lambda_{0,1}$  and  $z_{0,1}$  being the ultrasonic wavelength and path length in the wedge and the solid, respectively. It should be noted that Eqs. 5 through 7 as implemented in Eq. 4 are not expected to be quantitatively correct in this application to IGSCC inspection but should introduce roughly the correct frequency dependence for a specific transducer selection.

#### EXPERIMENTAL COMPARISONS

To test the validity of Eq. 4 as implemented using Eqs. 5-7, experiments were performed on a Ti-6Al-4V plate containing four approximately semi-elliptical EDM slots with depths ranging from 0.038 to 0.152 cm (0.015 to 0.060 in.) and surface-breaking lengths of 0.140 to 0.358 cm (0.055 to 0.141 in.). Measurements were performed in immersion using a 1.27 cm (0.50 in.) diameter unfocussed 5 MHz transducer oriented at a 19.2° angle relative to the sample surface to couple into a 45° shear wave in the plate. A corner reflection from the edge of the plate was used as the reference signal. A representative comparison of model predictions to experimental measurements is shown in Fig. 2, in which the frequency domain result of Eq. 4 has been Fourier transformed into the time domain. This figure compares results for the 0.114 cm (0.045 in.) deep slot. Qualitatively, the agreement in pulse shape, including the amplitude of the tip signal (the small precursor to the main signal feature) relative to the crack mouth signal, is quite good. Unfortunately, the signal amplitudes differ by an order of magnitude. Results from the other three slots were similar, except that for the 0.038 cm (0.015 in.) deep slot, neither the model nor experimental waveforms showed a distinct tip signal. Since the ultrasonic wavelength in the solid is approximately 0.064 cm (0.025 in.), the tip signal would not be expected to be resolved in time from the mouth signal. Investigations are currently under way to identify the cause of the amplitude discrepancy between model and experiment.

#### APPLICATION TO IGSCC SIZING

As an example of the practical application of the IGSCC model, we will illustrate its use by predicting the performance of two typical IGSCC sizing methods - the dB drop and pulse-arrival-time (PAT) techniques. The former method attempts to size a crack by first positioning a probe to achieve the maximum signal from the crack and then repositioning the probe to either side of the defect such that the signal is reduced by a specified amount. The defect height estimate is the distance between the latter two probe positions. The PAT method begins, once again, by maximizing the crack signal. For a typical IGSCC, this position will correspond to the probe position which directs the ultrasonic beam axis toward the crack mouth (corner trap). Next, the probe position is varied to maximize the crack tip signal. The crack height is then simply related to the time delay between these two maximized signals[2]. It is known that the dB-drop technique cannot work for a surface-breaking defect, since the primary signal feature in that case is the crack mouth reflection[2]. Thus the dB-drop technique only provides a measure of the ultrasonic beam width. The PAT method, on the other hand, does typically provide accurate height estimates. These statements have been verified by experimental tests[7].

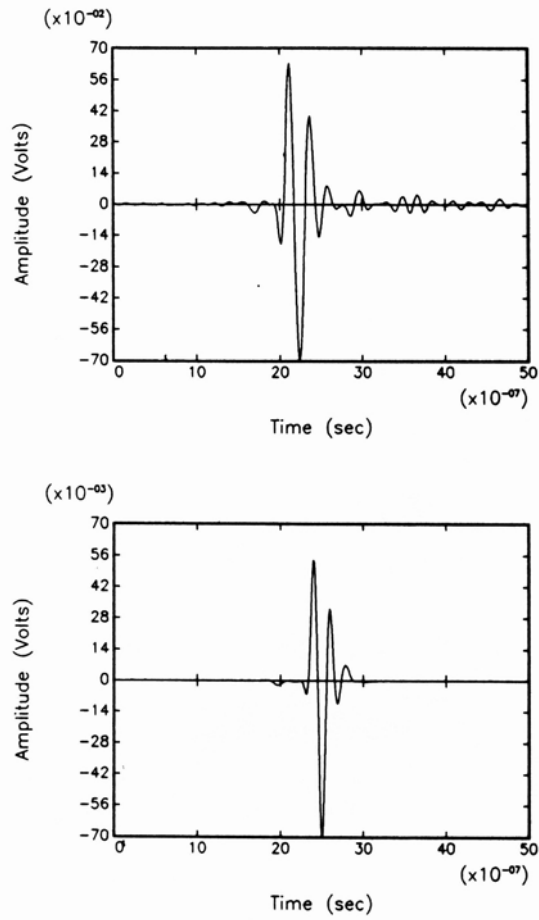


Fig. 2.  $45^{\circ}$  shear wave signals from a 0.045 in. deep semi-elliptical defect. (Top = experiment, bottom = model)

To simulate the sizing performance, the model was exercised for a set of branched cracks ranging in total depth from 0.318 to 2.286 cm (0.125 to 0.90 in.) for which the angle between branches was varied from zero to 90° and the ratio of stem height to crack height was varied from 0.5 to 0.99. The results of all simulations are shown in Figs. 3 (dB-drop) and 4 (PAT). The dB-drop method shows no correlation between estimated and actual IGSCC height, while the PAT technique exhibits an essentially perfect capability. Similar results were obtained previously using a 2-D Y-crack model[2], except that the PAT method showed some scatter in the estimated height for simulated IGSCC's of identical height but different "topologies" (e.g., different

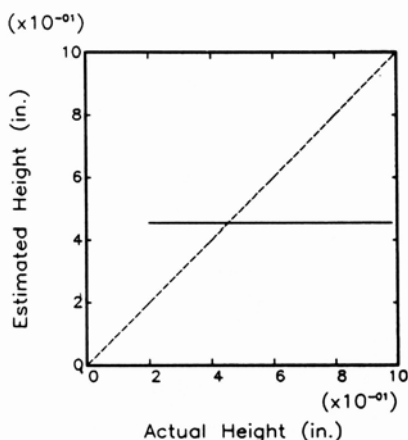


Fig. 3. Predicted sizing performance for dB-drop technique (solid line).

branch angles). The improvement in model accuracy illustrated in Fig. 4 is due to the ability in the 3-D model to approximate the crack opening displacement using the ultrasonic fields incident at an arbitrary user-specified point on the crack element (stem or branch). In the 2-D model, these fields were evaluated at the crack centroid. Thus, the signal from a branch, for example, would be maximized when the beam axis is directed toward the branch's centroid rather than toward the tip. Choosing the user-specified point to be the crack tip in the 3-D model causes the signals to be maximized when the beam axis strikes the tip, as is observed experimentally.

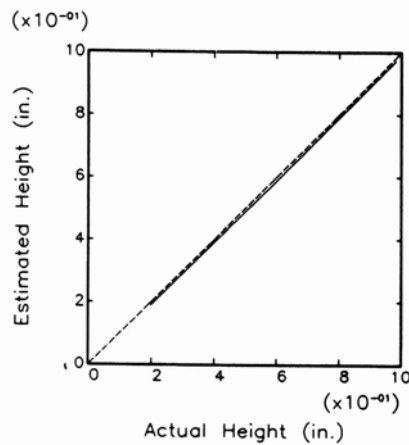


Fig. 4. Predicted sizing performance for P.A.T. technique (solid line).

#### SUMMARY

This report has described the implementation and application of a model for predicting the ultrasonic response from IGSCC's. There is still the need, however, for further model refinement, particularly to determine the source of an order of magnitude discrepancy between measured and model predicted signal amplitudes. Other model considerations which are warranted include development and implementation of more accurate ultrasonic beam models and scattering theories. Further practical considerations include the possibility of modeling the response from "geometrical" reflectors, such as a nearby weld, and the need to incorporate surface finish effects to allow simulation of inspection through cladding, etc. The future goal of this work is to develop a model-based tool for use in the design of new inspection techniques and configurations, the verification of their capability, the selection of alternative approaches, and the validation of existent techniques. The ability to synthesize simulated waveforms could also be of considerable value in training programs. Such a capability could thus offer a significant economic benefit in that it would allow NDE systems to be designed and evaluated using predictive approaches, rather than empirical methods relying upon extensive sample preparation and experimentation.

#### ACKNOWLEDGMENT

This work was sponsored by the Electric Power Research Institute under research project RP2687-1.

## REFERENCES

1. B. A. Auld, Wave Motion, 1, 1979, pp 3-10.
2. R. B. Thompson, T. A. Gray, J. D. Achenbach and K. Y. Hu, 1983, EPRI Report NP-3822.
3. R. B. Thompson, T. A. Gray, J. D. Achenbach and D. Budreck, final report for EPRI contract RP2687-1 (in press).
4. J. D. Achenbach and D. E. Budreck, these proceedings.
5. R. B. Thompson and E. F. Lopes, J. Nondestr. Eval., 4, 1984, pp. 107-123.
6. R. B. Thompson and T. A. Gray, J. Acoust. Soc Am. 74, 1983, pp. 1279-1290.
7. G. J. Dau and M. Behravesh, in Effective Nondestructive Examination for Pressurized Components, R. Nichols and G. J. Dau, eds., Applied Science Pub. Ltd. (in press).